

Cosmological Perturbation Theory and the Spherical Collapse model: Part III. The Velocity divergence field & the Ω dependence

Pablo Fosalba and Enrique Gaztañaga

IEEC- Institut d'Estudis Espacials de Catalunya, Research Unit (CSIC),
Edf. Nexus-201 - c/ Gran Capità 2-4, 08034 Barcelona, Spain

2 December 2024

ABSTRACT

Cosmological Perturbation Theory (PT) is a useful tool to study the cumulants of the density and velocity fields in the large scale structure of the Universe. In papers I & II of this series we saw that the Spherical Collapse (SC) model provides with the exact solution to PT at tree-level and gives a good approximation to the loop corrections (next to leading orders), indicating negligible tidal effects. Here, we derive predictions for the (smoothed) cumulants of the velocity divergence field $\theta \equiv \nabla \cdot \mathbf{v}$ for an irrotational fluid in the SC model. By comparing with the exact analytic results by Scoccimarro & Frieman (1996), it is shown that, at least for the unsmoothed case, the loop corrections to the cumulants of θ are dominated by tidal effects. However, most of the tidal contribution seems to cancel out when computing the hierarchical ratios, $T_J = \langle \theta^J \rangle / \langle \theta^2 \rangle^{J-1}$. We also extend the work presented in Papers I & II to give predictions for the cumulants of the density and velocity divergence fields in non-flat spaces. In particular, we show the equivalence between the *spherically symmetric* solution to the equations of motion in the SC model (given in terms of the density) and that of the Lagrangian PT approach (in terms of the displacement field). It is shown that the Ω dependence is very weak for both cosmic fields even at one-loop (a 10% effect at most), except for the overall factor $f(\Omega)$ that couples to the velocity divergence.

1 INTRODUCTION

One of the aims of modern Cosmology is to understand the origin and growth of the large scale structure as we observe it today. Cosmological Perturbation Theory (PT) has revealed to be a key analytic tool to make predictions about the cosmological matter density δ and velocity \mathbf{v} fields in the weakly non-linear regime (ie, when $v, \delta \lesssim 1$). However, most of the results derived so far are only applicable to the *unsmoothed* fields, Gaussian initial conditions (GIC) and flat space (ie, $\Omega = 1$ for a vanishing cosmological constant Λ). These results concern the tree-level (leading-order for GIC, see Peebles 1980, Fry 1984, Bernardeau 1992, hereafter B92) as well as loop corrections (higher-orders for GIC, cf Scoccimarro & Frieman 1996a, 1996b). Comparison with N-body simulations and observations made it necessary to incorporate the effects of smoothing in the PT calculations (Goroff et al. 1986, Juszkiewicz et al. 1993, Bernardeau 1994a, 1994b, Baugh, Gaztañaga, Efstathiou 1995, Gaztañaga & Baugh 1995). Further results were obtained for non-Gaussian IC in a number of papers (Fry & Scherrer 1994, Chodorowsky & Bouchet 1996) which allows to discriminate among models of structure formation (Silk & Juszkiewicz 1991, Gaztañaga & Mähönen 1996).

In Paper I (Fosalba & Gaztañaga 1998) and Paper II (Gaztañaga & Fosalba 1998) of this series it was shown that the *Spherical Collapse (SC) model gives the exact tree-level contribution to PT irrespective of the nature of the IC and the geometry of the universe*. The latter means that, when it comes to computing the one-point cumulants at tree-level, only the *spherically symmetric* solution to the equations of motion is relevant (see Paper I §2.7). This solution generates the *monopole* term, ν_n , ie the angle average of the kernels in Fourier space. As a result, the evolved density field is entirely determined by a local transformation of the linear density field alone, what we shall call a *local-density* transformation (see Paper I §2.5),

$$\delta = f(\delta_l) = \sum_{n=1}^{\infty} \frac{\nu_n}{n!} [\delta_l]^n. \quad (1)$$

Making use of this property we were able to present in Papers I & II results for Gaussian (GIC) and non-Gaussian IC (NGIC) respectively, for both the unsmoothed and smoothed fields (for a top-hat window). Furthermore, the SC model was used to make predictions beyond the tree-level in both cases which were shown to be in good agreement with N-body simulations up to the scales where PT

itself is expected to break down (see Paper I §4 and Paper II §3.3).

In this paper, we derive results for the peculiar velocity field \mathbf{v} which is the counterpart to the density field in the Newtonian equations of motion. The peculiar velocity field as traced by a population of galaxies has the potential advantage, with respect to the corresponding matter density, of being a better (or at least different) tracer of the corresponding underlying field. This is because galaxy velocities should follow the gravitational field regardless of their luminosity. These property has been proposed as a way to make predictions about the density parameter of the universe Ω (see Bernardeau 1994b) and references therein). In what follows we shall assume that the fluid is irrotational as is usually done in PT. The latter is a good approximation in the SC model as the nonlinear density field is given in terms of the linear field alone, for which, PT predicts a dilution of vorticity with the expansion. Within this approximation the velocity field is entirely determined by its divergence $\theta \equiv \nabla \cdot \mathbf{v}$. The cumulants (or connected moments) of the velocity divergence are defined as: $\langle \theta^J \rangle_c$ and the corresponding hierarchical ratios: $T_J = \langle \theta^J \rangle_c / \langle \theta^2 \rangle^{J-1}$. Results for the one-point cumulants of the velocity divergence field were given in Juszkiewicz 1993 for the skewness S_3 (at tree-level and GIC, alone). Bernardeau 1994a, 1994b (B94a,b hereafter) systematically derived the dependence of these statistical quantities on the initial power spectrum for a top-hat window function and the strong (overall) omega dependence (see B94b) to leading-order (tree-level) for GIC.

We shall also extend the work to non-flat spaces (ie, $\Omega \neq 1$ for a vanishing cosmological constant Λ) for the cumulants of both the density and velocity divergence fields. Curvature effects on the hierarchical amplitudes have been investigated in a number of papers: Martel & Freudling 1991, and Bouchet et al. 1992 obtained the (weak) Ω dependence of the skewness of the density field in the Lagrangian PT approach. Bernardeau 1994b, (B94b hereafter) numerically integrated the Ω -dependence of the skewness and kurtosis of the density and velocity fields. Exact analytic results, concerning the curvature-dependence of the skewness, were derived in Bouchet et al. 1995 (BCHJ95 hereafter) in Lagrangian PT and Catelan et al. 1995, in Euler space.

This paper is organized as follows. Section §2 presents the results for the velocity divergence field while in §3 results for the Ω dependence in the SC model are given. A discussion and the final conclusions is given in §4. Appendix §A provides the connection between the vertex generating function in PT and the SC equation for arbitrary Ω . Appendix §B gives an alternative derivation of the Ω dependence of the monopole in Lagrangian PT.

2 RESULTS FOR THE VELOCITY DIVERGENCE FIELD

In this section we apply our results from the SC model for the density field (see Papers I & II) to derive, the one-point cumulants for the velocity field in the quasi-linear regime. For the current analysis, we shall consider an irrotational fluid and, as a result, the velocity field is fully described by its divergence, $\theta \equiv \nabla \cdot \mathbf{v} / \mathcal{H}$, where $\mathcal{H}(\tau) = a(t)H(t)$ is the conformal Hubble parameter and $a(t)$ is the scale factor.

As mentioned above, this is a good approximation in the SC model as nonlinear dynamics are fully determined by the linear growth of perturbations for which the vorticity decays with time.

The velocity divergence is *locally* related to the linear density field through the continuity equation, which for an Einstein-deSitter space reads,

$$\dot{\delta} + (1 + \delta) \theta = 0, \quad (2)$$

so that the linear solution is $\theta_l = -\delta_l$. This way, introducing Eq.[1] above, we can obtain an analog local-transformation for the velocity divergence, say,

$$\theta = \sum_{k=1}^{\infty} \frac{\mu_k}{k!} \theta_l^k \quad (3)$$

where the *unsmoothed* μ_k coefficients are to be derived order by order in a perturbative expansion of the continuity equation. Thus one finds,

$$\begin{aligned} \mu_1 &= \nu_1 = 1 \\ \mu_2 &= 2(1 - \nu_2) = -\frac{26}{21} \simeq -1.24 \\ \mu_3 &= 3(\nu_3 - 3\nu_2 + 2) = \frac{142}{63} \simeq 2.25 \\ \mu_4 &= 4(-\nu_4 + 4\nu_3 + 3\nu_2^2 - 12\nu_2 + 6) \\ &= -\frac{236872}{43659} \simeq -5.42 \end{aligned} \quad (4)$$

and so on.

2.1 Smoothing effects

The smoothing effects for the velocity field for a top-hat window can be easily derived by applying similar arguments to those used for the density field (see Paper I §3.4 and B94b). In particular, the continuity equation ensures that the smoothed velocity divergence field is proportional to the unsmoothed one, $\hat{\theta} \sim \theta$ as induced by the sharp cut in the smoothed density field with respect to the unsmoothed one, $\hat{\delta} \sim \delta$. Moreover, the local character of the unsmoothed velocity divergence field (see above) tells us that $\theta \sim g[\theta_l]$. Now, from the linear continuity equation we get, $\hat{\theta}_l = -\hat{\delta}_l = -(\sigma_l/\hat{\sigma}_l) \delta_l = (\sigma_l/\hat{\sigma}_l) \theta_l$. Introducing the latter in the local transformation g which determines $\hat{\theta}$ we finally get,

$$\hat{\theta} \sim g\left[\frac{\sigma_l}{\hat{\sigma}_l} \hat{\theta}_l\right] \quad (5)$$

where \sim just means that the transformation is performed in Lagrangian space so that it has to be properly normalized when going back to Euler space (see Paper I §3.2).

For a power-law power spectrum $P(k) \sim k^n$, one finds (see Paper I),

$$\hat{\sigma}_l = \sigma_l (1 + \hat{\delta})^{-\gamma/6}. \quad (6)$$

where $\gamma = -(n + 3)$. As a result, the smoothed non-linear velocity divergence field is given by,

$$\hat{\theta}[\hat{\theta}_l] \sim \theta[\hat{\theta}_l(1 + \hat{\delta})^{\gamma/6}], \quad (7)$$

to be normalized when transforming back to Euler space in an analog way as is done with the density field (see Paper I §3.4). Notice that the latter results are formally equivalent

SC	Unsmoothed				Smoothed			
	$\gamma = 0$	$\gamma = -1$	$\gamma = -2$	$\gamma = -3$	$n = -3$	$n = -2$	$n = -1$	$n = 0$
$s_{2,4}^\theta$	10.97	7.98	5.61	3.84				
$-T_{3,0}$	3.71	2.71	1.71	0.71				
$-T_{3,2}$	3.86	-0.20	-0.37	1.12				
$T_{4,0}$	27.41	13.65	4.55	0.12				
$T_{4,2}$	131.06	29.97	17.49	15.30				

Table 1. Values for the higher-order perturbative contributions in the SC model for the unsmoothed ($n = -3$) and smoothed ($n = -2, -1, 0$) velocity fields.

to those provided by B94a for the smoothed fields in Euler space although, here, we work in Lagrangian space.

According to the latter transformation, the first smoothed coefficients of the velocity field read,

$$\begin{aligned} \overline{\mu_2} &= \frac{1}{3}(-6\nu_2 + 6 - \gamma) = \mu_2 - \frac{\gamma}{3} \\ \overline{\mu_3} &= \frac{1}{4}(4\mu_3 - 5\mu_2\gamma + \gamma^2) \\ \overline{\mu_4} &= \mu_4 - \frac{20}{9}\gamma\mu_3 - \gamma\mu_2^2 + 2\gamma^2\mu_2 - \frac{8}{27}\gamma^3, \end{aligned} \quad (8)$$

and so forth, where in the latter equalities we have applied the identities given by (4).

Combining Eqs.[3],[4] and [8], we can derive the smoothed cumulants for the velocity divergence up to an arbitrary perturbative order in an Einstein-deSitter universe for a top-hat window and a power-law power spectrum, for GIC & NGIC.

2.2 Gaussian initial conditions

Following the notation introduced in Paper I §4, we shall use for the perturbative expansion of the variance,

$$\sigma_\theta^2 = \langle \hat{\theta}^2 \rangle = \sum_i s_{2,i}^\theta \sigma_l^i \quad (9)$$

where $s_{2,1} \equiv 1$ and the subscript in the coefficients labels the order of the perturbative expansion. Note that σ_l denotes the *rms* fluctuation of the linear *density* field. As for the hierarchical amplitudes we keep the above notation with the added labeling of the order of the moment J , that defines the T_J coefficients,

$$T_J \equiv \frac{\langle \hat{\theta}^J \rangle_c}{\langle \hat{\theta}^2 \rangle^{J-1}} = \sum_i T_{J,i} \sigma_l^i \quad (10)$$

As we did with the density field (see Paper I §4), we shall denote the leading order contributions (ie, the tree-level for GIC) by $T_J^{(0)}$.

2.2.1 SC results

For GIC the odd terms in the perturbative expansion vanish, thus,

$$\begin{aligned} \sigma_\theta^2 &= \sigma_l^2 + s_{2,4}^\theta \sigma_l^4 + s_{2,6}^\theta \sigma_l^6 + \dots \\ T_J^G &= T_{J,0} + T_{J,2} \sigma_l^2 + T_{J,4} \sigma_l^4 + \dots \end{aligned} \quad (11)$$

For the variance, skewness and kurtosis of $\hat{\theta}$ [for a top-hat window and a scale-free power spectrum, where $n = -(\gamma + 3)$] in an Einstein-deSitter universe, we find:

$$\begin{aligned} s_{2,4}^\theta &= \frac{1613}{147} + \frac{415}{126}\gamma + \frac{11}{36}\gamma^2 \\ -T_{3,0} &\equiv -T_3^{(0)} = \frac{26}{7} + \gamma \\ -T_{3,2} &= \frac{43712}{11319} + \frac{8926}{1323}\gamma + \frac{55}{18}\gamma^2 + \frac{10}{27}\gamma^3 \\ T_{4,0} &\equiv T_4^{(0)} = \frac{12088}{441} + \frac{338}{21}\gamma + \frac{7}{3}\gamma^2 \\ T_{4,2} &= \frac{10934570594}{83432349} + \frac{56796896}{305613}\gamma + \frac{2613829}{23814}\gamma^2 \\ &+ \frac{31067}{1134}\gamma^3 + \frac{1549}{648}\gamma^4. \end{aligned} \quad (12)$$

Table 1 displays the results for the smoothed field for different values of the spectral index.

To compare our results to those available in the literature we should focus on the *unsmoothed* one-point cumulants,

$$\begin{aligned} \sigma_\theta^2 &\approx \sigma_l^2 + 10.97\sigma_l^4 + \mathcal{O}(\sigma_l^6) \\ -T_3 &\approx 3.71 + 3.86\sigma_l^2 + \mathcal{O}(\sigma_l^4) \\ T_4 &\approx 27.41 + 131.06\sigma_l^2 + \mathcal{O}(\sigma_l^4). \end{aligned} \quad (13)$$

The results from the exact PT in the diagrammatic approach derived in Scoccimarro & Frieman (1996a) are,

$$\sigma_\theta^2 \approx \sigma_l^2 + 1.08\sigma_l^4 + \mathcal{O}(\sigma_l^6) \quad (14)$$

and the first corrective term for T_3 was viewed to strongly depend on the spectral index due to non-local effects: $-2.58 \gtrsim T_{3,2} \gtrsim -4.64$, for $2 \geq n \geq -2$. Thus, our local value $T_{3,2} = -3.86$, is compatible with the average of the above non-local values. For the variance however, the corrective term seems to be dominated by non-local (tidal) effects which cut down non-linearities in an order of magnitude, unlike the case of the density field (see Paper I §4.1). The situation might be different for the smoothed cumulants, as we have seen (in Papers I&II) that for $n \simeq -1.5$ tidal effects seem to cancel out.

Fig 1 depicts the departures from the tree-level contributions for different values of the spectral index as the linear variance grows. Notice that, in general, the smoothing effects tend to suppress nonlinear contributions in accordance with the trend observed for the density field (see Paper I Table 2 & Paper II Table 1).

2.2.2 SSZA results

The Zel'dovich Approximation (ZA hereafter, see Zel'dovich 1970) formally corresponds to the first order in the Lagrangian approach to PT (see Appendix B for details) which is based in a perturbative expansion of the Jacobian that relates the Lagrangian to the Eulerian coordinates. It assumes

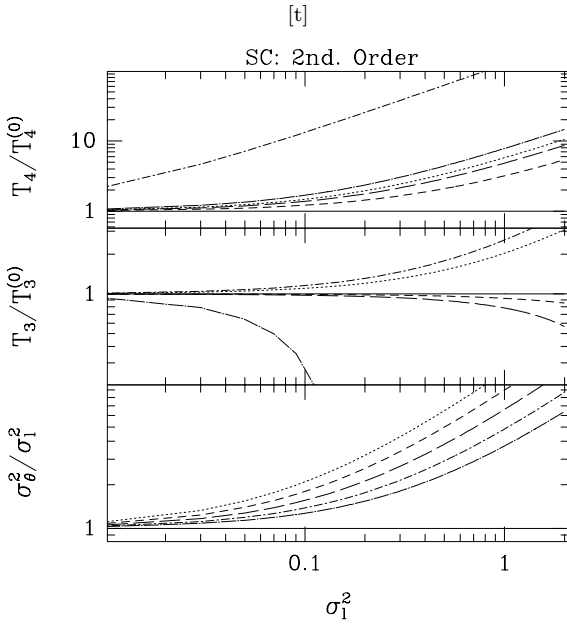


Figure 1. Departures from the tree-level up to one loop as a function of the linear rms fluctuation. The variance, skewness and kurtosis of the velocity divergence predicted by the SC model are shown for different values of the spectral index: the dotted line shows the $n = -3$ (unsmoothed) case, and the short-dashed ($n = -2$), long-dashed ($n = -1$), dot short-dashed ($n = 0$), dot long-dashed ($n = 1$) depict the behavior for the smoothed field. The solid line shows the tree-level values.

SSZA	Unsmoothed		Smoothed	
	$\gamma = 0$	$\gamma = -1$	$\gamma = -2$	$\gamma = -3$
	$n = -3$	$n = -2$	$n = -1$	$n = 0$
$s_{2,4}^\theta$	6.56	4.47	3	2.14
$-T_{3,0}$	2	1	0	-1
$-T_{3,2}$	2.07	1.43	2	1.57
$T_{4,0}$	8	1.67	0	3
$T_{4,2}$	38.44	17.40	6	-0.78

Table 2. Values for the higher-order perturbative contributions in the SSZA for the unsmoothed ($n = -3$) and smoothed ($n = -2, -1, 0$) velocity fields.

that the particle positions in comoving coordinates follow straight trajectories in Lagrangian space. In this section we proceed and give the results for the *spherically symmetric* solution to the equations of motion within the Zel'dovich Approximation (SSZA hereafter, see Paper I §5). In particular, we give estimates of the cumulants for the *smoothed* velocity divergence (for a top-hat window and a power-law power spectrum) in an Einstein-deSitter universe,

$$s_{2,4}^\theta = \frac{59}{9} + \frac{43}{18} \gamma + \frac{11}{36} \gamma^2$$

$$\begin{aligned}
 -T_{3,0} &\equiv -T_3^{(0)} = 2 + \gamma \\
 -T_{3,2} &= \frac{56}{27} + 2\gamma + \frac{31}{18}\gamma^2 + \frac{10}{27}\gamma^3 \\
 T_{4,0} &\equiv T_4^{(0)} = 8 + \frac{26}{3}\gamma + \frac{7}{3}\gamma^2 \\
 T_{4,2} &= \frac{346}{9} + \frac{3392}{81}\gamma + \frac{5447}{162}\gamma^2 \\
 &+ \frac{2459}{162}\gamma^3 + \frac{1549}{648}\gamma^4
 \end{aligned} \tag{15}$$

thus, the *unsmoothed* cumulants ($\gamma = 0$) show the following scaling,

$$\begin{aligned}
 \sigma_\theta^2 &\approx \sigma_l^2 + 6.56\sigma_l^4 + \mathcal{O}(\sigma_l^6) \\
 -T_3 &\approx 2 + 2.07\sigma_l^2 + \mathcal{O}(\sigma_l^4) \\
 T_4 &\approx 8 + 38.44\sigma_l^2 + \mathcal{O}(\sigma_l^4).
 \end{aligned} \tag{16}$$

This should be compared to the *unsmoothed* results from the exact PT in the diagrammatic approach up to the one-loop contribution (see Scoccimarro & Frieman 1996a),

$$\begin{aligned}
 \sigma_\theta^2 &\approx \sigma_l^2 + 0.73\sigma_l^4 + \mathcal{O}(\sigma_l^6) \\
 -T_3 &\approx 2 + 1.64\sigma_l^2 + \mathcal{O}(\sigma_l^4) \\
 T_4 &\approx 8 + 17.58\sigma_l^2 + \mathcal{O}(\sigma_l^4)
 \end{aligned} \tag{17}$$

illustrating again the point made above (see §2.2.1): tidal effects dominate the variance of the velocity field and make non-linear effects small, what can not be recovered within the local SSZA dynamics. Again here, the situation might be different for the smoothed cumulants, as we have seen (in Papers I&II) that for $n \simeq -1.5$ tidal effects seem to cancel out. Despite this limitation intrinsic to our *local* approximation, we see that tidal effects almost cancel their contributions to the reduced cumulants. The latter renders the SSZA approximation a good estimator of these quantities in line with the results obtained previously for the density field.

Table 2 shows the results for the smoothed velocity divergence field in the SSZA for different values of spectral index. Fig 2 displays deviations from the tree-level contributions for different values of n as the linear variance approaches unity.

2.3 Non-Gaussian initial conditions

For NGIC, no additional equations need to be solved as all the information relevant for the computation of the one-point cumulants is encoded in the Gaussian tree-level (see Paper I §2.9). The perturbation expansion is worked out in an analog way to that for GIC, the only difference being the order at which the dominant terms appear as induced by the scaling properties of the IC (see Paper II §3). We represent the different orders in the expansion as we did for the GIC above Eq.[9]-[10].

We will assume, as a generic case, that the NGIC are dimensional: $\langle \theta^J \rangle \propto \langle \theta^2 \rangle^{J/2}$, and we will define the corresponding initial amplitudes as:

$$B_J \equiv B_J^\theta = \frac{\langle \hat{\theta}_l^J \rangle_c}{\langle \hat{\theta}^2 \rangle^{J/2}}, \tag{18}$$

not to be confused here with the corresponding coefficients for the density fields. The latter scaling induces different ordering in the perturbative series as compared to the GIC

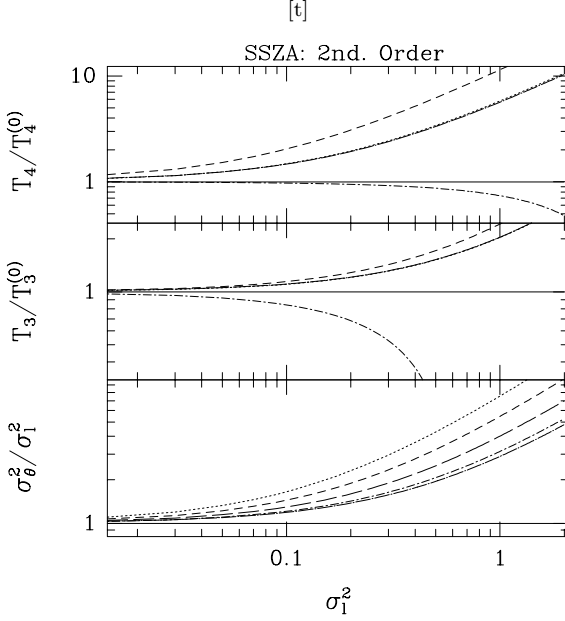


Figure 2. Same as Fig 1 for the SSZA. Note that the line $n = -1$ is not shown for T_3 and T_4 since the tree-level hierarchical amplitudes vanish. The values $n = -3$ (unsmoothed) and $n = -1$ lead to the same scaling properties for the skewness and kurtosis so the corresponding lines overlap.

one. In particular, we find the following results for the first contributions to the cumulants filtered with a top-hat (assuming a power-law spectrum) and an Einstein-deSitter background,

$$\begin{aligned}
 s_{2,3}^\theta &= -B_3 \left(\frac{T_3^G}{3} + 1 \right) \\
 -T_{3,-1} &\equiv -T_3^{(0)} = B_3 \\
 -T_{3,0} &= -T_3^G + 2 \left(\frac{T_3^G}{3} + 1 \right) B_3^2 - \left(\frac{T_3^G}{2} + 1 \right) B_4 \\
 T_{4,-2} &\equiv T_4^{(0)} = B_4 \\
 T_{4,-1} &= -4T_3^G B_3 + (3 + T_3^G) B_3 B_4 \\
 &\quad - \left(\frac{2}{3} T_3^G + 1 \right) B_5,
 \end{aligned} \tag{19}$$

where T_J^G correspond to the *tree-level* PT results for GIC. The *unsmoothed* one-point cumulants (setting $\gamma = 0$ in the Gaussian coefficients above) we find:

$$\begin{aligned}
 s_{2,3}^\theta &= \frac{5}{21} B_3 \sigma_l^3 \\
 -T_{3,-1} &\equiv -T_3^{(0)} = B_3 \\
 -T_{3,0} &= \frac{26}{7} - \frac{10}{21} B_3^2 + \frac{6}{7} B_4 \\
 T_{4,-2} &\equiv T_4^{(0)} = B_4 \\
 T_{4,-1} &= -\frac{104}{7} B_3 - \frac{5}{7} B_3 B_5 + \frac{31}{21} B_5
 \end{aligned} \tag{20}$$

We can compare these results to those from exact PT, derived in Protogeros and Scherrer 1997, which give for T_3 for the unsmoothed fields (setting the overall Ω dependence,

$f(\Omega) = 1$ for a flat universe),

$$\begin{aligned}
 -T_3 &= \frac{\langle \delta_l^3 \rangle}{\sigma_l^4} + \frac{26}{7} - \frac{10}{21} \frac{\langle \delta_l^3 \rangle^2}{\sigma_l^6} + \frac{6}{7} \frac{\langle \delta_l^4 \rangle}{\sigma_l^4} \\
 &+ \frac{4}{7} \left[3 \frac{I[\xi_3^0]}{\sigma_l^4} - 4 \frac{\langle \delta_l^3 \rangle I[\xi_3^0]}{\sigma_l^6} \right] + \mathcal{O}(\sigma_l),
 \end{aligned} \tag{21}$$

where $I[\xi_3^0]$ and $I[\xi_4^0]$ denote some integral of the initial 3 and 4-point functions which are intrinsically *non-local* terms (see Eq.[27] in Paper II). Thus, replacing $T_3^G = -26/7$ and $B_J = \langle \theta_l^J \rangle_c / \sigma_l^J$ in our expressions (see Eq.[20] above), we find, as we did with the density field (see Papers I & II), that the SC model gives the exact result up to some tidal (non-local) terms which results in a small contribution to the hierarchical amplitudes. This smallness is partially due to the fact that they enter as a difference between integrals of the initial J -point functions which are generically of the same order, at least for the density field (see Paper II §3.4).

For the smoothed fields however, our results must be taken as a prediction since there are no explicit results for non-Gaussian initial conditions. For some general implicit results, which depend on the initial J -point functions for the smoothed T_3 , see Protogeros & Scherrer (1997). The latter should contain all our local terms when given in a somewhat more explicit fashion.

Figs 3 and 4 show the evolved variance, skewness and kurtosis as they depart from their first perturbative contributions $T_J^{(0)}$. As we pointed out in the case for the density field (see Paper I §3.1 Figs. 1 & 2), the variance of the velocity divergence is seen to be dominated by the initial conditions in the second perturbative contribution (only terms $\sim B_J$ appear) while gravity takes over once the third perturbative contribution is included. The latter is realized by the enhancement of the non-linear variance with respect of the linear one (at least, for large values of the linear *rms* density fluctuation) in accordance with the expectation from the SC model for GIC. The hierarchical amplitudes show the same coupling to the initial conditions as for the density field so all perturbative contributions are taken over by the initial conditions. In Figures 3 & 4 we have taken the initial *dimensional* coefficients $B_J \approx 1$, in analogy to the case for the density field (see Paper II §3.1), though we find no physical motivation by which they should be comparable. However, we have checked that the qualitative behavior of the statistical quantities and thus the overall picture is not significantly altered if we change those amplitudes by an order of magnitude ie, our conclusions are robust.

3 THE Ω DEPENDENCE IN THE SC MODEL

3.1 The Ω dependence in the density field

3.1.1 The SC model approach

In the previous papers (see Papers I & II) we assumed a spatially flat (Einstein-deSitter) universe with a vanishing cosmological constant Λ , in order to derive our predictions for the one-point cumulants. Although it is the simplest analytic approach and there are strong theoretical arguments which favor an $\Omega = 1, \Lambda = 0$ universe (e.g., standard inflationary models), it remains to be seen whether or not this is actually so.

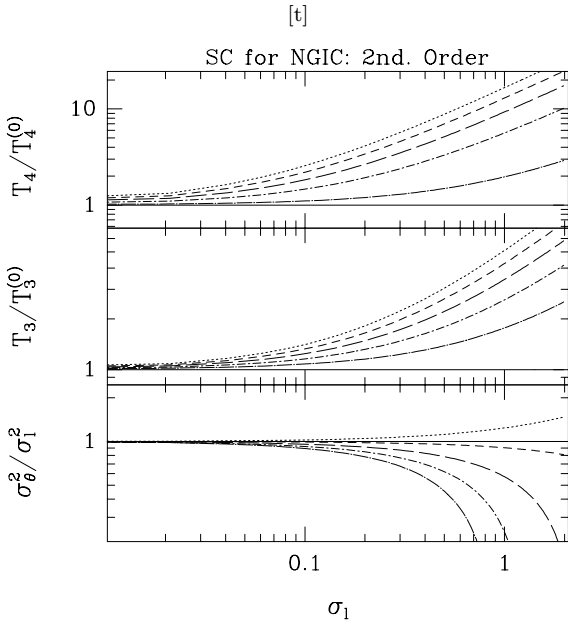


Figure 3. Same as Fig 1 for non-Gaussian dimensional initial conditions. We assume $B_J \approx 1$.

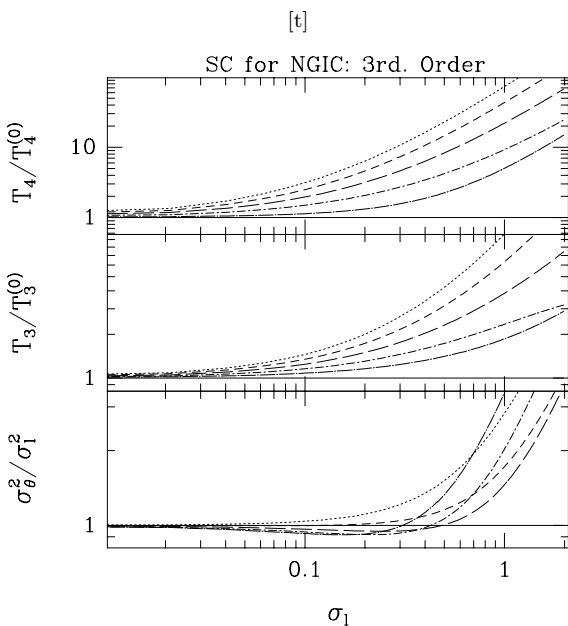


Figure 4. Same as Fig 3 when the 3rd. perturbative contributions are taken into account in the evolved one-point cumulants.

In our calculations, we have neglected the effect of a non-vanishing cosmological constant Λ . However, detailed analyses have shown that the dependence of the cumulants on this parameter is extremely weak anyway, at least for a flat universe $\Omega + \Lambda = 1$ (see Lahav et al. 1991, BCHJ95).

We showed in Paper I that in the general case of a perturbative approach to estimate the leading order (tree-level) contribution to the cumulants it is not necessary to calculate the full kernels F_n , but only the *monopole* contribution, $\nu_n \equiv \langle F_n \rangle$, which corresponds to the spherically symmet-

ric (angle) average. Thus the values of ν_n can be determined by finding the spherically symmetric solution to the equations of motion. We also show that for gravity, this solution is given by the spherical collapse (SC). The proof (§3.1 in Paper I) holds irrespective of the geometry of the universe, ie, for arbitrary Ω (which shows explicitly through the Friedmann equation: $4\pi G\bar{\rho} = 3/2\Omega H^2$). Therefore, we can write the local non-linear transformation introduced in flat space (see Paper I, §3 Eq.[33]) and write,

$$\delta = \sum_{i=1}^{\infty} \frac{\nu_n(\Omega)}{n!} [\delta_i]^n. \quad (22)$$

where the $\nu_n(\Omega)$ coefficients are a generalization of the flat-space monopole amplitudes ν_n in non-flat FRW geometries. This can be readily obtained by considering the parametric solution to the SC dynamics in an open universe ($\Omega < 1$):

$$\begin{aligned} \delta_l &= D(\psi) \left[\left(\frac{\sinh \theta - \theta}{\sinh \psi - \psi} \right)^{2/3} - 1 \right] \\ \delta &= \left(\frac{\cosh \psi - 1}{\cosh \theta - 1} \right)^3 \cdot \left(\frac{\sinh \theta - \theta}{\sinh \psi - \psi} \right)^2 - 1 \end{aligned}$$

for $\delta_l > -D(\psi)$, and

$$\begin{aligned} \delta_l &= -D(\psi) \left[\left(\frac{-\sin \theta + \theta}{\sinh \psi - \psi} \right)^{2/3} + 1 \right] \\ \delta &= \left(\frac{\cos \psi - 1}{-\cos \theta + 1} \right)^3 \cdot \left(\frac{\sin \theta - \theta}{\sinh \psi - \psi} \right)^2 - 1, \end{aligned} \quad (23)$$

for $\delta_l < -D(\psi)$, with

$$\begin{aligned} D(\psi) &= \frac{9}{2} \frac{\sinh \psi (\sinh \psi - \psi)}{(\cosh \psi - 1)^2} - 3 \\ \psi &= \cosh^{-1} \left(\frac{2}{\Omega} - 1 \right), \end{aligned} \quad (24)$$

where $D(\psi)$ is the growing mode of the linear density contrast (see also B92). In order to get the solution for an $\Omega > 1$ universe, the transformation $\psi \rightarrow i\psi$ must be performed in the above expressions. This way, the $\nu_n(\Omega)$ coefficients may be numerically integrated by expanding the parametric solutions around $\delta_l = 0$. An alternative derivation of the Ω dependence of the Gaussian tree-level was presented by Bernardeau (1992) in terms of the vertex generating function. In Appendix A1 we present the connection between the latter and the SC equation for arbitrary Ω .

A good fit to the above results can be obtained by realizing that in Lagrangian PT (see §B) the Ω -dependence of the hierarchical amplitudes only appears beyond the first perturbative contribution (which corresponds to the ZA). As the larger the density parameter is, the smaller the S_J parameters are (this is a monotonous behavior at least within the range $10 \gtrsim \Omega \gtrsim 0$), one is led to the simplest possible ansatz for $S_J(\Omega)$ which is of the form,

$$S_J(\Omega) = S_J^{ZA} + B \Omega^{-\alpha}$$

being α and B positive constants. What is more, imposing that for $\Omega = 1$ one must recover the well-known Einstein-deSitter values, one gets,

$$S_J(\Omega) = S_J^{ZA} + (S_J^{\Omega=1} - S_J^{ZA}) \Omega^{-\alpha} \quad (25)$$

so that α is the only parameter to be fitted by inspection in a log-log plot of the numerically integrated solutions. In particular, for the cosmologically favored range $2 \gtrsim \Omega \gtrsim 0.1$, we obtain the following numerical fits for the tree-level hierarchical amplitudes,

$$\begin{aligned} S_3(\Omega) &= 3\nu_2(\Omega) \approx \frac{34}{7} + \frac{6}{7} (\Omega^{-3/91} - 1) \\ S_4(\Omega) &= 4\nu_3(\Omega) + 12\nu_2(\Omega)^2 \\ &\approx \frac{60712}{1323} + \frac{20728}{1323} (\Omega^{-1/27} - 1) \end{aligned} \quad (26)$$

from which we derive the fits for $\nu_2(\Omega)$ and $\nu_3(\Omega)$. Moreover, replacing these unsmoothed coefficients in the general expressions for the smoothed $\bar{\nu}_k$ (since the smoothing effects were derived independent of the geometry of the universe, see Paper I §3.4), we get at tree level,

$$\begin{aligned} S_3(\Omega) &= 3\bar{\nu}_2(\Omega) \approx \frac{34}{7} + \frac{6}{7} (\Omega^{-3/91} - 1) + \gamma \\ S_4(\Omega) &= 4\bar{\nu}_3(\Omega) + 12\bar{\nu}_2(\Omega)^2 \\ &\approx \frac{60712}{1323} + \frac{20728}{1323} (\Omega^{-1/27} - 1) + \\ &+ \frac{62}{3}\gamma + \frac{7}{3}\gamma^2 + 4\gamma (\Omega^{-3/91} - 1). \end{aligned} \quad (27)$$

Moreover, the numerical fits for the $\nu_n(\Omega)$ can be used to derive the corresponding approximate Ω -dependences for the σ -corrections to the cumulants as they carry all the dynamical information in the SC model (see Paper I, §2.6). Fig 5 shows the departures from the tree-level amplitudes for different values of Ω . As shown there, the dependence is rather weak and only for values of Ω close to zero are the predictions a 10% greater than those for flat space.

We have also explored the Ω -dependence of the non-linear variance. Making use of the fits derived for the $\nu_k(\Omega)$ above, we find for the first non-linear correction (one-loop),

$$\begin{aligned} s_{2,4} &= \frac{1909}{1323} + \frac{143}{126}\gamma + \frac{11}{36}\gamma^2 - \frac{10}{49}(\Omega^{-6/91} - 1) \\ &+ \frac{5182}{1323}(\Omega^{-1/27} - 1) + \frac{1}{21}(11\gamma - 64)(\Omega^{-3/91} - 1). \end{aligned} \quad (28)$$

From the above result we estimate that the non-flat ($\Omega < 1$) variance to one-loop can be a 10% greater at most (for $\sigma_l < 1$), than the flat space value, similarly to what we found for the S_J amplitudes. We stress nevertheless that the SC result for the variance only gives an accurate approximation to the exact PT result (and the N-body predictions) around $n \simeq -1.5$ ($\gamma \simeq -1.5$), where tidal forces yield a negligible contribution (see Paper I §4.2).

The general trend observed in the hierarchical amplitudes for the density contrast in the non-linear regime, according to the SC model, is that, the lower the density parameter is, the higher the amplitudes are. This fact may be easily explained in terms of the growing modes that rule the gravitational evolution of the density contrast: it seems that the hydrodynamic effect according to which the expansion of the universe drags the growth of the growing mode in the linear regime (large scales for a given time) also dominates further stages of the evolution (quasi-linear scales). Since in a low density universe the hydrodynamic effects are larger, the growing modes collapse faster what leads to the observed excess in the one-point cumulants as Ω approaches zero in comparison with the behavior for larger values of the density parameter (see Fig 5).

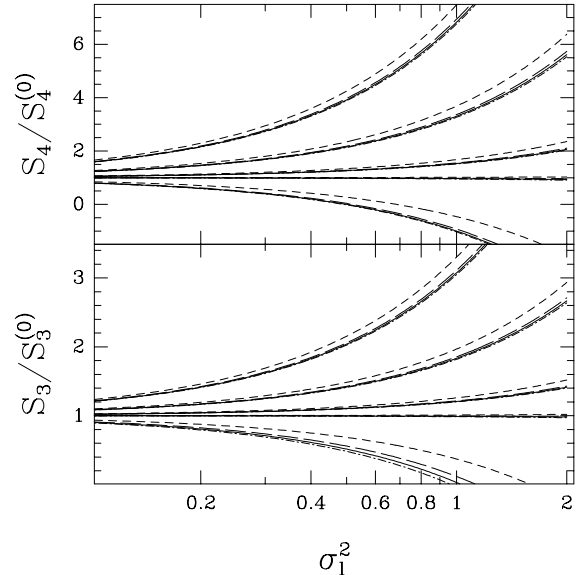


Figure 5. Predictions for the departures from the tree-level contributions in the skewness and kurtosis for non-flat universes. The solid line corresponds to the flat-space prediction while the short-dashed, long-dashed and dot-dashed lines give the behavior for models with $\Omega = 0, 0.4, 2$ respectively. It is seen how the weak dependence with the density parameter in the non-linearities makes it hard to distinguish them from those of the flat-space unless Ω approaches zero. The upper group of lines correspond to $n = -3$ while lower groups of lines show the smoothed cases: from $n = -2$ to $n = 1$ (bottom group of lines).

3.1.2 The Lagrangian PT approach

An independent derivation of the approximated Ω -dependence in the hierarchical amplitudes of the density and velocity fields is provided by the Lagrangian PT approach (see Moutarde et al. 1991, BCHJ95). Since the *spherically symmetric* solution to the equations of motion gives the exact tree-level contribution to PT (see Paper I §2.5 & Paper II §2.3), we shall impose the *spherically symmetric* condition on the relevant equations of motion in Lagrangian PT to get the exact tree-level as well in that formalism. Lagrangian PT is formulated in terms of the perturbation of the original trajectory in Lagrangian space q , so that the perturbative series is built by expanding the Jacobian $J = |\partial x/\partial q|$ of the transformation between Lagrangian and Euler coordinates $x(t, q) = q + \Psi(t, q)$ (being Ψ the so-called displacement field). This is equivalent to expanding the density contrast in Lagrangian space since,

$$\delta = \frac{\rho}{\bar{\rho}} - 1 = \frac{1}{J} - 1. \quad (29)$$

In this framework, the derivatives of the displacement field $\Psi_{i,j}$ play the role of the smallness parameter in the perturbative expansion, instead of the linear density contrast δ_l as it was the case for the SC model. By imposing *spherical symmetry* in the growth of perturbations we set $\Psi_{1,1} = \Psi_{2,2} = \Psi_{3,3} = \Psi_{k,k}$ (being zero otherwise). So for all perturbative orders, it holds that, $J^{(n)} \propto [J^{(1)}]^n$ (see §B for details). This is the key point in the connection with the SC model as it explicitly shows that all the perturba-

tive orders can be expressed as powers of the linear one as was the case for the expansion in terms of the linear density field in the SC model. In other words, we can build a local-density transformation (see Eq.[1]) in Lagrangian PT from the *spherically symmetric* solution to the equations of motion whose coefficients (the g_k functions, see §B) carry the same information than the ν_k ones in the SC model. Identifying the linear terms in both expansions we can formally relate all higher perturbative orders one by one, from which we can derive the relations between the coefficients (g_k with ν_k) that determine the one-point statistics in both formalisms.

In particular (See Appendix A2), we get for the first coefficients,

$$\begin{aligned}\nu_2 &= \frac{2}{3} \left(2 - \frac{g_2}{g_1^2} \right) \\ \nu_3 &= \frac{2}{9} \left(10 - 12 \frac{g_2}{g_1^2} + \frac{g_{3a}}{g_1^3} + 6 \frac{g_{3b}}{g_1^3} \right).\end{aligned}\quad (30)$$

Once we relate both *unsmoothed* coefficients ν_k with g_k , we can simply apply all previously given results for the SC model by rewriting the expressions appropriately in terms of the new g_k coefficients. It is important to stress the equivalence between the SC model predictions in Lagrangian and Euler space at tree-level (see Paper I §3.2). Thus only beyond tree-level (next-to-leading terms in PT) there are differences between the SC model formulated in Euler space and the *spherically symmetric* approach to Lagrangian PT.

Furthermore, the equivalence between both formalisms (the SC model and the Lagrangian PT) in Lagrangian space allows to induce a fit to the Ω -dependence of the g_k functions from that of the ν_k ones. We can compare the fits given by BCHJ95 with our fits for the cumulants to see which ones match better the numerical results. Although the exact analytic expression for g_1 & g_2 are known (see BCHJ95), no exact results are available for higher-orders, so we shall focus on their numerical fits for the cosmologically favored parameter space for Ω and work out the predictions. According to BCHJ95, near $\Omega = 1$, good fits are provided by the following factors,

$$\begin{aligned}\frac{g_2}{g_1^2} &\approx -\frac{3}{7} \Omega^{-2/63} \\ \frac{g_{3a}}{g_1^3} &\approx -\frac{1}{3} \Omega^{-4/77} \\ \frac{g_{3b}}{g_1^3} &\approx \frac{5}{21} \Omega^{-2/35}.\end{aligned}\quad (31)$$

Combining Eqs.[30] & [31] we get the fits to the $\nu_k(\Omega)$ coefficients from Lagrangian PT approach. The smoothing effects for a top-hat window can be incorporated as described in Paper I §3.4. The resulting smoothed coefficients $\nu_k(\Omega)$ in terms of the unsmoothed ones $\nu_k(\Omega)$, are given by Eq.[A3] in Paper I. Replacing them in the smoothed S_J amplitudes yields, for a power-law spectrum $\gamma = -(n + 3)$,

$$\begin{aligned}S_3(\Omega) &= 3\bar{\nu}_2 \approx \frac{34}{7} + \frac{6}{7} (\Omega^{-2/63} - 1) + \gamma \\ S_4(\Omega) &= 4\bar{\nu}_3 + 12\bar{\nu}_2^2 \\ &\approx \frac{60712}{1323} + \frac{48}{49} (\Omega^{-4/63} - 1) + \frac{80}{63} (\Omega^{-2/35} - 1) \\ &- \frac{8}{27} (\Omega^{-4/77} - 1)\end{aligned}$$

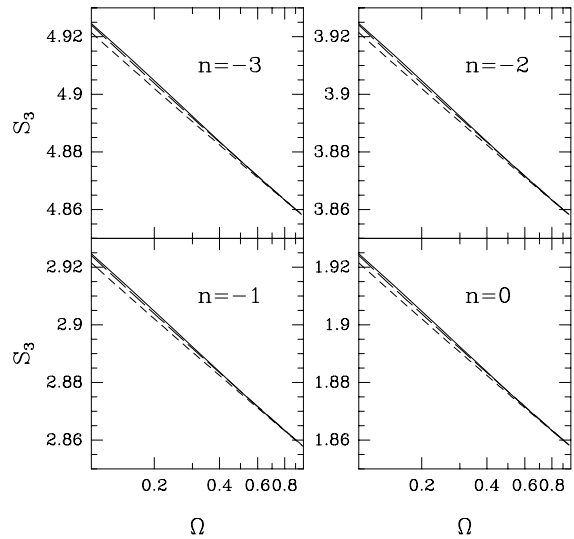


Figure 6. Comparison between the exact (numerically integrated) S_J amplitudes at tree-level (solid line) and the numerical fits to the Ω -dependence for the open models. The short-dashed line shows the SC predictions making use of the BCHJ95 fits in the context of the Lagrangian PT, while the long-dashed line gives the fits to the SC model solutions.

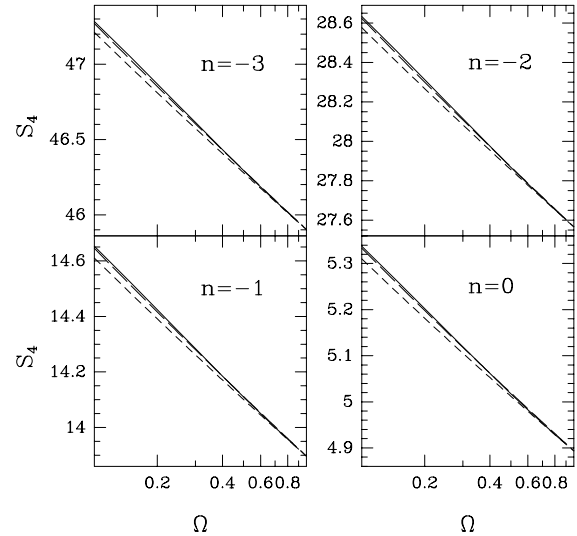


Figure 7. Same as Fig 6 for the kurtosis.

$$+ \frac{62}{3} \gamma + \frac{7}{3} \gamma^2 + \left(\frac{96}{7} + 4\gamma \right) \cdot (\Omega^{-2/63} - 1). \quad (32)$$

Figs 6 and 7 show the Ω dependence of the skewness and kurtosis of the density field which is shown to be very weak, as expected. In particular we compare the exact solution for the Ω dependence to the generic fits for the SC model based on Eq.[25] on one hand, and the above results derived from the *spherically symmetric* solution to the Lagrangian PT approach on the other hand. Our fits are slightly more accu-

rate than those given by BCHJ95, which nevertheless only underestimate the skewness and kurtosis by 1% at most.

3.2 The Ω dependence in the velocity field

In this section, we extend the results obtained in §2 to the case where the density parameter $\Omega \neq 1$. In general, an overall factor $f(\Omega) = d \log D(t)/d \log a(t)$ (see Eq.[36] below), couples to the velocity divergence in the continuity equation for a non-flat space, what we shall call the *strong* Ω -dependence, which scales in the moments of the velocity divergence $\langle \theta^J \rangle \propto f(\Omega)^J$. Therefore, for the cumulants, one expects

$$T_J(\Omega) \approx \frac{1}{f(\Omega)^{J-2}} T_J(\Omega = 1), \quad (33)$$

with $f(\Omega) \approx \Omega^{0.6}$, provided one assumes a vanishing cosmological constant $\Lambda = 0$ (see Peebles 1980). Nonetheless, there is also a *weak* dependence on the density parameter that modulates the dominant (strong) dependence (see Bouchet *et al.* 1994 and B94a). This dependence is induced by the density field in a non-flat space and is obtained through the equation of motion when the generalized coefficients of the density field $\nu_k(\Omega)$ replace those for flat-space in Eq.[4]. However, as commented above (see §3), the fits to the $\nu_k(\Omega)$ coefficients can be derived either in the SC model approach or in the Lagrangian PT approach since they are formally equivalent (see Appendix B for details).

From the fits to the SC model approach for the density field (see §3.1.1), we induce the following approximate Ω dependences for the velocity divergence field whenever $2 \gtrsim \Omega \gtrsim 0.1$,

$$\begin{aligned} -T_3 f(\Omega) &= 3 \overline{\mu_2(\Omega)} \approx \left[\frac{26}{7} + \frac{12}{7} (\Omega^{-3/91} - 1) + \gamma \right] \\ T_4 f(\Omega)^2 &= 4 \overline{\mu_3(\Omega)} + 12 \overline{\mu_2(\Omega)}^2 \\ &\approx 4 \left[\frac{3022}{441} + \frac{12}{49} (\Omega^{-6/91} - 1) + \frac{169}{42} \gamma + \frac{7}{12} \gamma^2 \right. \\ &\quad \left. + \frac{13}{7} \gamma (\Omega^{-3/91} - 1) \right]. \end{aligned} \quad (34)$$

Alternatively, when we make use of the $\nu_k(\Omega)$ as they are derived from the Lagrangian PT approach (see Appendix B) we get,

$$\begin{aligned} -T_3 f(\Omega) &\approx \left[\frac{26}{7} + \frac{12}{7} (\Omega^{-2/63} - 1) + \gamma \right] \\ T_4 f(\Omega)^2 &\approx \left[\frac{12088}{441} + \frac{192}{49} (\Omega^{-4/63} - 1) + \frac{80}{21} (\Omega^{-2/35} - 1) \right. \\ &\quad - \frac{8}{9} (\Omega^{-4/77} - 1) + \frac{338}{21} \gamma + \frac{7}{3} \gamma^2 \\ &\quad \left. + \frac{4}{7} (22 + 13 \gamma) \cdot (\Omega^{-2/63} - 1) \right], \end{aligned} \quad (35)$$

where the strong Ω -dependence $f(\Omega) = d \log D(\psi)/d \log a$ (where a is the scale factor and $D(\psi)$ is the growing mode of the linear density contrast) can be exactly integrated and yields for $\Omega < 1$,

$$f(\Omega) = \frac{3 \operatorname{sech}(\psi/2) ((2 + \Omega) \psi - 6 \sqrt{1 - \Omega})}{\Omega (9 \sinh(\psi/2) + \sinh(3\psi/2) - 6 \psi \cosh(\psi/2))}$$

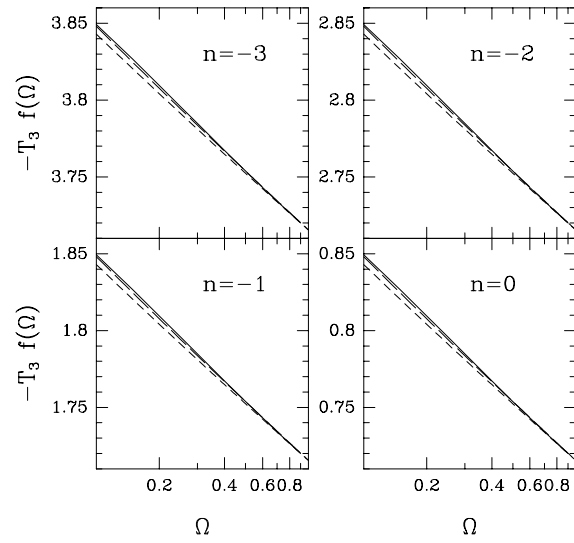


Figure 8. Same as Fig 6 for T_3 .

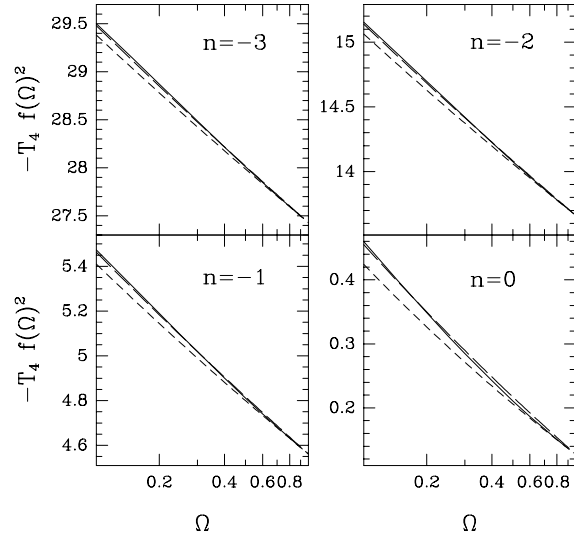


Figure 9. Same as Fig 6 for T_4 .

while for $\Omega > 1$, it has the form,

$$f(\Omega) = \frac{3 \operatorname{sec}(\psi/2) ((2 + \Omega) \psi - 6 \sqrt{\Omega - 1})}{\Omega (9 \sin(\psi/2) + \sin(3\psi/2) - 6 \psi \cos(\psi/2))} \quad (36)$$

where, $\psi = \cosh^{-1}(2/\Omega - 1)$. However, the fit $f(\Omega) \approx \Omega^{3/5}$ is a good approximation for open models as originally put forward by Peebles 1980. Other more accurate fits are $f(\Omega) \approx \Omega^{13/22}$ for open models and $f(\Omega) \approx \Omega^{13/23}$ for closed models within the range $2 \gtrsim \Omega \gtrsim 1$.

In Figs 8 and 9 we plot the weak Ω -dependences derived from the two independent fits, against the exact behavior numerically integrated. It shows that both fits are in agree-

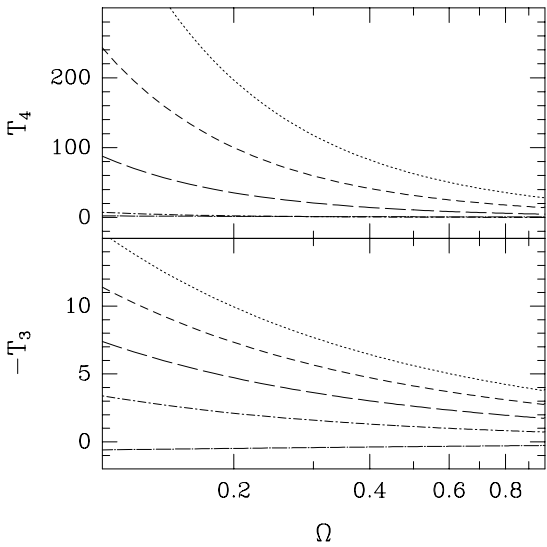


Figure 10. Values for the skewness and kurtosis of the velocity divergence at tree-level for open models. The smoothing effects strongly suppress the Ω -dependence which increases with the order of the hierarchical amplitudes T_J . The dotted line displays the $n = -3$ (unsmoothed) case while lower lines depict the smoothed cases for $n = -2, -1, 0, 1$ respectively from top to bottom.

ment with the exact solution within 1% and 5% for T_3 and T_4 respectively.

In Fig 10 we display the Ω -dependence (combining both the strong and weak ones) in the skewness and kurtosis of the velocity divergence for different values of the spectral index. There are two main features that arise in these dependences. First, though the relative variation of T_J with Ω increases with the smoothing effects (larger spectral index), the absolute variation decreases with them what makes it more plausible to probe Ω from lower values of the spectral index (which effectively means looking at small scales). Secondly, the dependence with the density parameter increases with J , so that looking at higher-order moments of the velocity divergence in the galaxy catalogues seems to be a promising test for determining Ω .

We stress that the behavior of the closed models is just an extrapolation of the one seen for the open models near $\Omega = 1$, so that only small changes arise in the range $10 \gtrsim \Omega \gtrsim 1$, as compared to the case of the open models.

3.3 The Ω -dependence for non-Gaussian initial conditions

For both cosmic fields (density or velocity) the Ω -dependence with NGIC can be recovered by combining in a straight forward way the results we have presented so far.

This can be done by noticing that the NGIC results are given in terms of the Gaussian tree-level amplitudes (see §2.3 for the velocity and Paper II for the density). Thus, to obtain the Ω -dependence one just have to substitute the Gaussian tree-level amplitudes (ie S_J^G or T_J^G) with the corresponding Ω -dependent amplitudes, given above in Eq.[27] or Eq.[34].

For example the variance σ^2 of the density field with NGIC is:

$$\begin{aligned} \sigma^2 &= \sigma_l^2 + s_{2,3} \sigma_l^3 + \dots \\ s_{2,3} &= \left(\frac{13}{21} + \frac{6}{21} (\Omega^{-3/91} - 1) + \frac{\gamma}{3} \right) B_3^0 \end{aligned} \quad (37)$$

where $B_3^0 \equiv \langle \delta_0^3 \rangle / \langle \delta_0^2 \rangle^{3/2}$ corresponds to the amplitude of the (dimensional) skewness of the initial density field.

4 DISCUSSION AND CONCLUSIONS

For Gaussian initial conditions (GIC), we found in Paper I, that the Spherical Collapse (SC) model gives very accurate predictions for the hierarchical amplitudes S_J in the perturbative regime, as compared to the results derived by Scoccimarro & Frieman (1996a, 1996b) for the exact PT in the diagrammatic approach (see Paper I §4.1). We also compared the predictions for the higher-order moments from the SC model to those measured in CDM and APM-like N-body simulations, and they turned out to be in very good agreement in all cases up to the scales where $\sigma_l \approx 1$, supporting our view that the tidal effects only have a marginal contribution to the reduced cumulants (see Paper I §4.2 & §4.3). For Non-Gaussian initial conditions (NGIC) the SC recovers all terms given by the exact PT for the variance, σ , skewness, S_3 , and kurtosis, S_4 , up to non-local integrals, involving n -point initial functions that arise as a result of the coupling between the asymmetric initial conditions with the tidal forces (see Paper II §3.4). The measured higher-order moments in the N-body simulations with NGIC (with dimensional, texture-like, scaling) turned out to be in good agreement with predictions from the SC model (see Paper II §3.3), what gives further support to the domain of applicability of the SC model in PT.

In this paper, we have extended the work presented in Papers I & II and have applied the SC model in Lagrangian space to study the predictions for the cumulants of the velocity divergence field as well as the Ω -dependence of the one-point cumulants in cosmological PT. We provide with the results for the velocity field up to one loop (first correction to the leading term). However, the loop predictions turned out not to be as accurate as those for the density field, suggesting they are dominated by tidal effects. This can be explicitly seen in the variance, see (Eqs.[13]-[14]) where the first non-linear correction to the linear contribution is only accurate in the order of magnitude with respect to the exact result for the unsmoothed field. The situation might be different for the smoothed cumulants, as we have seen (in Papers I&II) that for $n \simeq -1.5$ tidal effects seem to cancel out, at least in the case of the density. The SC loop predictions for the *reduced* cumulants, are in better agreement with those obtained in the exact PT. The latter suggests a cancellation of the tidal contributions in line with the behavior found for the density field.

As for the Ω -dependence, we showed that the SC model is the exact solution at tree-level for the one-point cumulants for arbitrary density parameter, Ω (see also §A for a demonstration in the context of B92). This property was explicitly used to derive the Ω -dependence of the cumulants

at tree-level for the density and velocity divergence fields. As an independent check to our results we worked out the *spherically symmetric* solution to Lagrangian PT which was shown to be equivalent to our solution within the SC model in Lagrangian space as well (see §B). This way we were able to compare available fits in Lagrangian PT at tree-level to our fits within the SC model. We found a good agreement between these results as well as with the exact numerically integrated solution: within 1% for the density field and 5% for the velocity divergence (see Figs. 6, 7 & 8,9 respectively).

We also present as a new result the Ω -dependence of the one-loop corrections in the SC approximation, for GIC and NGIC. We show that both the variance and S_J increase as Ω decreases ($\Omega < 1$). For the variance with GIC, this trend is in the line shown by fitting formulas and numerical simulations (Peacock & Dodds 1996) and reflects the slowed-down growth of perturbations on large scales for high density FRW universes. Although this effect is small (less than 10% for $\sigma < 1$) the SC results should be accurate for $n \simeq -1.5$, and could therefore be useful when compared to observations of the large scale structure in the weakly non-linear regime.

ACKNOWLEDGEMENTS

This work has been supported by CSIC, DGICYT (Spain), project PB96-0925, and CIRIT, grant GR94-8001.

5 REFERENCES

Baugh, C.M., Gaztañaga, E., Efstathiou, G., 1995, MNRAS, 274, 1049

Bernardeau, F., 1992, ApJ, 392, 1 (B92)

Bernardeau, F., 1994a, A&A 291, 697 (B94a)

Bernardeau, F., 1994b, ApJ, 433, 1 (B94b)

Bernardeau, F., 1994c, ApJ, 427, 51

Bouchet, F. R., Juszkiewicz, R., Colombi, S., 1992 Ap. J., 394, 5

Bouchet, F. R., Colombi, S., Hivon, E., Juszkiewicz, R., 1995 A & A, 296, 575 (BCHJ95)

Catelan, P., Lucchin, F., Matarrese, S., Moscardini, L., 1995, MNRAS, 276, 39

Chodorowski, M.J., Bouchet, F.R., 1996, MNRAS, , 279, 557

Fosalba, P., Gaztañaga, E., 1997, submitted to MNRAS, astro-ph/9712095 (Paper I).

Fry, J.N., 1984, ApJ, 279, 499

Fry, J.N., Scherrer, 1994, R.J., ApJ, 429, 1

Gaztañaga, E. & Baugh, C.M., 1995, MNRAS, 273, L1

Gaztañaga, E. & Mähönen, P., 1996, Ap. J., 462, L1

Gaztañaga, E., Fosalba, P., 1997, submitted to MNRAS, astro-ph/9712263 (Paper II).

Juszkiewicz, R., Bouchet, F.R., Colombi, S., 1993 Ap. J., 412, L9

Lahav, O., Lilje, P.B., Primack, J.R., Rees, M.J., 1991, MNRAS, 251, 128

Moutarde, F., Alimi, J.M., Bouchet, F.R., Pellat, R., Raman, A., 1991 ApJ, 382, 377

Peacock, J.A., Dodds, S.J., 1996, MNRAS, 280, L19.

Peebles, P.J.E., 1980, *The Large Scale Structure of the Universe*: Princeton University Press, Princeton

Peebles, P.J.E., 1990, ApJ, 365, 27

Protogeros, Z.A.M., Scherrer, R.J., 1997, MNRAS, 286, 223

Scoccimarro, R., Frieman J., 1996a, ApJS, 105, 37

Scoccimarro, R., Frieman J., 1996b, ApJ, 473, 620

Silk J., Juszkiewicz, R. 1991, Nature 353, 386

Zel'dovich, Ya.B., 1970. A & A, 5, 84

APPENDIX A: GAUSSIAN TREE-LEVEL WITH ARBITRARY Ω

We want to show here, in the framework of Bernardeau (1992) calculations, that the equations of motion that govern the tree-level amplitudes for Gaussian initial conditions in a FRW universe with arbitrary density parameter Ω , are those of the SC dynamics.

Let us first introduce the vertex generating function which is defined as (see B92),

$$\mathcal{G}_F(\tau) = \sum_{k=1}^{\infty} \frac{\nu_k}{k!} (-\tau)^k$$

where $\nu_k = \langle F^{(n)} \rangle_c^n$, for a generic field F and the superscript n in the average denotes that all tree-level contributions come through diagrams that have n external lines (see B92 for details). According to B92, the equations of motion for \mathcal{G}_δ have the form,

$$\begin{aligned} \left[a \frac{\partial}{\partial a} + f(a)\tau \frac{\partial}{\partial \tau} \right] \mathcal{G}_\delta(a, \tau) &= -[1 + \mathcal{G}_\delta(a, \tau)] \mathcal{G}_{\Delta\Phi}(a, \tau) \\ \left[a \frac{\partial}{\partial a} + f(a)\tau \frac{\partial}{\partial \tau} \right] \mathcal{G}_{\Delta\Phi}(a, \tau) + \frac{1}{3} \mathcal{G}_{\Delta\Phi}^2(a, \tau) &= \\ - \left[\frac{2\nu - 1}{\nu} + \frac{d \log \nu}{d \log a} \right] \mathcal{G}_{\Delta\Phi}(a, \tau) - \frac{3}{2} \Omega \mathcal{G}_\delta(a, \tau) \end{aligned} \quad (\text{A1})$$

with, Φ is the peculiar velocity potential, $f(a) \equiv d \log D(a)/d \log a$, and $\nu \equiv d \log a/d \log t = H t$, where t is the comoving time. First, as we want to recover the equations of motion in terms of the density contrast and the velocity divergence, we have to assume that the tree-level, $\mathcal{G}_\delta(a, \tau) = \delta$, as pointed out by B94 although there it was restricted to flat-space. Replacing the latter identity in the continuity equation (2) leads to $\mathcal{G}_{\Delta\Phi} = \theta \equiv \nabla \cdot \mathbf{v}/f(a) H$ provided we introduce the comoving time derivative in the way,

$$\frac{d}{dt} \equiv H \left(a \frac{\partial}{\partial a} + f(a)\tau \frac{\partial}{\partial \tau} \right). \quad (\text{A2})$$

Substituting this into (A1), we get

$$\ddot{\delta} + 2H\dot{\delta} - \frac{4}{3} \frac{\dot{\delta}^2}{(1+\delta)} = \frac{3}{2} \Omega H^2 \delta (1+\delta) = 4\pi G \bar{\rho} \delta (1+\delta), \quad (\text{A3})$$

where in the first equality we have made use of the equation of motion, $\dot{H} = -(1 + \Omega/2) H^2$ valid for a $\Lambda = 0$ universe, while the second equality follows from the Friedmann equation. Equation (A3) is exactly the equation of motion in the SC model (see Paper I §3.1).

On the other hand, as in the SC model the evolved density field is given by a local-density transformation of the kind,

$$\delta = f(\delta_l) = \sum_{n=1}^{\infty} \frac{c_n}{n!} \delta_l^n, \quad (\text{A4})$$

from the above equivalence between the vertex generating function and the density field from the SC model at tree-level,

$$\delta(\delta_l) = \mathcal{G}_\delta(a, -\tau), \quad (\text{A5})$$

it follows that $c_k(\Omega) = \nu_k(\Omega)$ ie, the coefficients of the local-density transformation are those of the SC model for a FRW universe with arbitrary Ω .

APPENDIX B: THE OMEGA DEPENDENCE FROM THE SC MODEL IN LAGRANGIAN PT

In this section we give a brief account of the Lagrangian PT which is based on an expansion of particle trajectories around the initial positions. We proceed and show the formal equivalence of the latter to the SC model in Lagrangian space. This result along with the available fits to the Lagrangian PT found by Bouchet *et al.* 1995 (BCHJ95 hereafter) allows to extend their results for the skewness to the kurtosis of the smoothed density and velocity fields.

Lagrangian PT contains the ZA as the first order of the perturbative series. Higher-orders were considered by Moutarde *et al.* 1991 what was later generalized by Bouchet *et al.* 1992. Our analysis here essentially follows the steps of BCHJ95 were the perturbative analysis was extended up to the third order.

We start by introducing the density contrast and relating it to the displacement field, i.e., the perturbation around the original trajectory in Lagrangian space,

$$\delta = \frac{\rho}{\bar{\rho}} - 1 = \frac{1}{J} - 1,$$

where J is the jacobian of the transformation between real (Euler) and Lagrangian space, $x(t, q) = q + \Psi(t, q)$,

$$\begin{aligned} J_{ij} &= \frac{\partial x_i}{\partial q^j} = \delta_{ij} + \Psi_{i,j} \\ J &= \left| \frac{\partial x}{\partial q} \right|, \end{aligned}$$

being Ψ_i the component of the displacement field along the i direction.

Expanding J and, consequently, Ψ_i in a perturbative series,

$$\begin{aligned} J &= 1 + \epsilon J^{(1)} + \epsilon^2 J^{(2)} + \dots \\ \Psi &= \epsilon \Psi^{(1)} + \epsilon^2 \Psi^{(2)} + \dots \end{aligned} \quad (\text{B1})$$

and rewriting J in terms of the perturbative contributions from the displacement field, we have,

$$J = 1 + \epsilon K^{(1)} + \epsilon^2 (k^{(2)} + L^{(2)}) + \epsilon^3 (k^{(3)} + L^{(3)} + M^{(3)}) + \dots \quad (\text{B2})$$

(see also Eq.[17] in Bernardeau 1994c) where the invariant scalars K, L, M are,

$$\begin{aligned} K &= \nabla \cdot \Psi = \sum_i \Psi_{i,i} \\ L &= \frac{1}{2} \sum_{i,j} (\Psi_{i,i} \Psi_{j,j} - \Psi_{i,j} \Psi_{j,i}) \\ M &= \det[\Psi_{i,j}] \end{aligned} \quad (\text{B3})$$

form which the first perturbative orders are read off,

$$\begin{aligned} K^{(m)} &= \sum_i \Psi_{i,i}^{(m)} \\ L^{(2)} &= \frac{1}{2} \sum_{i \neq j} (\Psi_{i,i}^{(1)} \Psi_{j,j}^{(1)} - \Psi_{i,j}^{(1)} \Psi_{j,i}^{(1)}) \\ L^{(3)} &= \sum_{i \neq j} (\Psi_{i,i}^{(2)} \Psi_{j,j}^{(1)} - \Psi_{i,j}^{(2)} \Psi_{j,i}^{(1)}) \\ M^{(3)} &= \det[\Psi_{i,j}^{(1)}]. \end{aligned}$$

The fluid equations of motion in Lagrangian space for a collisionless fluid can be written down in the simple form (see BCHJ95 for details),

$$J(\tau, q) \nabla \ddot{x} = \beta(\tau) [J(\tau, q) - 1], \quad (\text{B4})$$

where $d\tau \propto a^{-2} dt$, and the dot denotes time derivatives with respect to τ , while,

$$\beta(\tau) = \frac{6}{\tau^2 + k(\Omega)}, \quad (\text{B5})$$

with $k(\Omega)$ is a function of the geometry of the universe,

$$\begin{aligned} k(\Omega = 1) &= 0 \\ k(\Omega < 1) &= -1 \\ k(\Omega > 1) &= +1. \end{aligned}$$

The conformal time parameter $\tau = t^{-1/3}$ in a flat universe and goes like $\tau = |1 - \Omega|^{-1/2}$, for non-flat universes. Equation [B4] has a unique solution provided the fluid is irrotational $\nabla \times \ddot{x} = 0$, what we shall assume in the following.

Introducing the perturbative series in the equations of motion (B4), one finds as generic solutions to the perturbed equations of motion for an irrotational fluid,

$$\begin{aligned} K^{(1)}(\tau, q) &= g_1(\tau) K^{(1)}(\tau_i, q) \\ K^{(2)}(\tau, q) &= g_2(\tau) K^{(2)}(\tau_i, q) \\ K^{(3)}(\tau, q) &= g_{3a}(\tau) M^{(3)}(\tau_i, q) + g_{3b}(\tau) L^{(3)}(\tau_i, q), \end{aligned} \quad (\text{B6})$$

The first two orders are separable, unlike the third one, where two independent growing modes have to be taken into account. The above expression shall be taken as a definition of the g_k functions which encode the Ω dependence of the jacobian J , and thus that of the equations of motion in Lagrangian PT.

We now impose the *spherical symmetry* in the growth of perturbations which, in terms of the displacement field reads,

$$\begin{aligned} \Psi_{1,1} &= \Psi_{2,2} = \Psi_{3,3} = \Psi_{k,k} \\ \Psi_{i,j} &= 0 \quad \text{for } i \neq j. \end{aligned} \quad (\text{B7})$$

Applying these simple properties on the perturbative series of the jacobian we find,

$$\begin{aligned} K^{(1)}(\tau, q) &= 3 \Psi_{k,k}^{(1)}(\tau, q) = 3 g_1(\tau) \Psi_{k,k}^{(1)}(\tau_i, q), \\ K^{(2)}(\tau, q) &= 3 g_2(\tau) \Psi_{k,k}^{(1)2}(\tau_i, q) \\ L^{(2)}(\tau, q) &= 3 g_1^2(\tau) \Psi_{k,k}^{(1)2}(\tau_i, q) \\ K^{(3)}(\tau, q) &= (g_{3a}(\tau) + g_{3b}(\tau)) \Psi_{k,k}^{(1)3}(\tau_i, q) \\ L^{(3)}(\tau, q) &= 6 g_2(\tau) g_1(\tau) \Psi_{k,k}^{(1)3}(\tau_i, q) \end{aligned}$$

$$M^{(3)}(\tau, q) = g_1^3(\tau) \Psi_{k,k}^{(1)3}(\tau_i, q), \quad (\text{B8})$$

where we have made use of the fact that $K^{(2)}(\tau_i, q) = L^{(2)}(\tau_i, q)$ (see BCHJ95) which yields $\Psi_{k,k}^{(2)}(\tau_i, q) = \Psi_{k,k}^{(1)2}(\tau_i, q)$. Replacing the latter expressions in the perturbative orders of the jacobian one gets,

$$\begin{aligned} J^{(1)}(\tau, q) &= 3g_1(\tau) \Psi_{k,k}^{(1)}(\tau_i, q) \\ J^{(2)}(\tau, q) &= 3(g_1^2(\tau) + g_2(\tau)) \Psi_{k,k}^{(1)2}(\tau_i, q) \\ J^{(3)}(\tau, q) &= (g_{3a}(\tau) + 6g_{3b}(\tau) \\ &+ 6g_2(\tau)g_1(\tau) + g_1^3(\tau)) \Psi_{k,k}^{(1)3}(\tau_i, q). \end{aligned} \quad (\text{B9})$$

On the other hand, the unsmoothed transformation of the evolved density contrast in the SC model reads,

$$\delta = \delta_l + \frac{\nu_2}{2} \delta_l^2 + \frac{\nu_3}{3!} \delta_l^3 + \dots$$

while the analog expansion in terms of the jacobian gives,

$$\begin{aligned} \delta &= -\epsilon J^{(1)} + \epsilon^2 (J^{(1)2} - J^{(2)}) \\ &+ \epsilon^3 (-J^{(1)3} + 2J^{(1)}J^{(2)} - J^{(3)}) + \dots \end{aligned}$$

from which we see that the linear term is just $\delta_l = -\epsilon J^{(1)}$, and all perturbative orders can be expressed as powers of the linear term, since, $J^{(n)} \propto [J^{(1)}]^n$ in the same way $\delta^{(n)} \propto [\delta_l]^n$ in the SC model.

Identifying in the same way the higher-orders one by one (in powers of ϵ) and replacing the expressions for the $J^{(i)}$ according to (B9), we arrive at,

$$\begin{aligned} \nu_2 &= \frac{2}{3} \left(2 - \frac{g_2}{g_1^2} \right) \\ \nu_3 &= \frac{2}{9} \left(10 - 12 \frac{g_2}{g_1^2} + \frac{g_{3a}}{g_1^3} + 6 \frac{g_{3b}}{g_1^3} \right). \end{aligned} \quad (\text{B10})$$

Making use of these coefficients we immediately obtain the tree-level amplitudes for the skewness and kurtosis of the density field in terms of the g_k functions which in turn incorporate the Ω dependence,

$$\begin{aligned} S_3 &= 3\nu_2 = 4 - 2 \frac{g_2}{g_1^2} \\ S_4 &= 4\nu_3 + 12\nu_2^2 \\ &= \frac{8}{9} \left(34 - 36 \frac{g_2}{g_1^2} + 6 \left(\frac{g_2}{g_1^2} \right)^2 + \frac{g_{3a}}{g_1^3} + 6 \frac{g_{3b}}{g_1^3} \right). \end{aligned} \quad (\text{B11})$$

The expression for S_3 was already derived in BCHJ95 so the latter expressions extend their results to the kurtosis in a simple fashion. An immediate extension of the latter results to the *smoothed* fields is achieved by applying the expressions for the smoothed coefficients of the local non-linear transformation that describes the spherical collapse $\overline{\nu_k}$ (see section about smoothing effects in Paper I),

$$\begin{aligned} S_3 &= 3\overline{\nu_2} = 4 + \gamma - 2 \frac{g_2}{g_1^2} \\ S_4 &= 4\overline{\nu_3} + 12\overline{\nu_2}^2 \\ &= \frac{1}{9} \left[272 + 150\gamma + 21\gamma^2 - 12(24 + 7\gamma) \frac{g_2}{g_1^2} \right] \end{aligned}$$

$$+ 48 \left(\frac{g_2}{g_1^2} \right)^2 + 8 \frac{g_{3a}}{g_1^3} + 48 \frac{g_{3b}}{g_1^3} \right], \quad (\text{B12})$$

where the ZA (or the SSZA in our spherically symmetric approach), which corresponds to the first perturbative order in the Lagrangian approach, is recovered by setting $g_k = 0$, i.e., the Ω -independent term.

Though the exact analytic expressions for g_2/g_1^2 are known (see BCHJ95), no exact results are available for g_{3a}/g_1^3 and g_{3b}/g_1^3 , so we shall focus on the numerical fits for the cosmologically favored parameter space for Ω and work out the predictions. According to BCHJ95, near $\Omega = 1$ good fits are provided by the following factors,

$$\begin{aligned} \frac{g_2}{g_1^2} &\approx -\frac{3}{7} \Omega^{-2/63} \\ \frac{g_{3a}}{g_1^3} &\approx -\frac{1}{3} \Omega^{-4/77} \\ \frac{g_{3b}}{g_1^3} &\approx \frac{5}{21} \Omega^{-2/35}. \end{aligned} \quad (\text{B13})$$

Replacing the above dependences in the skewness and kurtosis we finally get the fits to the smoothed S_J amplitudes given by Eq.[32].

Similarly, we can derive the corresponding fits to the *weak* Ω -dependence in Lagrangian PT (see §B) for the skewness and kurtosis of the velocity divergence just by recalling the relationship between the unsmoothed coefficients of the local transformations for the density and velocity field provided by Eq.[4], and the expressions for the smoothed coefficients in terms of the unsmoothed ones provided by Eq.[8].

The smoothed T_3 and T_4 then read,

$$\begin{aligned} -T_3(\Omega) f(\Omega) &= 2 + \gamma - 4 \frac{g_2}{g_1^2} \\ T_4(\Omega) f(\Omega)^2 &= \frac{1}{3} \left[24 + 26\gamma + 7\gamma^2 - 4(22 + 13\gamma) \frac{g_2}{g_1^2} \right. \\ &\quad \left. + 64 \left(\frac{g_2}{g_1^2} \right)^2 + 8 \frac{g_{3a}}{g_1^3} + 48 \frac{g_{3b}}{g_1^3} \right], \end{aligned} \quad (\text{B14})$$

where the overall factor $f(\Omega)$ gives the strong dependence on the density parameter given by Eq.[36]. Introducing the fits given by BCHJ95 for the density field in the latter expressions, we obtain their approximated Ω -dependences given by Eq.[35].